Impact of sea ice on air-sea CO$_2$ exchange – A critical review of polar eddy covariance studies

Jennifer Watts [a,*], Thomas G. Bell [b], Karen Anderson [c], Brian J. Butterworth [d], Scott Miller [e], Brent Else [f], Jamie Shutler [a]

[a] Centre for Geography and Environmental Science, University of Exeter, Penryn, Cornwall, UK
[b] Plymouth Marine Laboratory, Plymouth, Devon, UK
[c] Environment and Sustainability Institute, University of Exeter, Penryn, Cornwall, UK
[d] University of Wisconsin-Madison, Madison, WI, USA
[e] Atmospheric Sciences Research Centre, University of Albany (State University of New York), USA
[f] Department of Geography, University of Calgary, Canada

ARTICLE INFO

ABSTRACT

Sparse *in situ* measurements and poor understanding of the impact of sea ice on air-sea gas exchange introduce large uncertainties to models of polar oceanic carbon uptake. The eddy covariance technique can be used to produce insightful air-sea gas exchange datasets in the presence of sea ice, but results differ between studies. We present a critical review of historical polar eddy covariance studies and can identify only five that present comparable flux datasets. Assessment of ancillary datasets, including sea-ice coverage and type and air-sea concentration gradient of carbon dioxide, used to interpret flux datasets (with a specific focus on their role in estimating and interpreting sea ice zone gas transfer velocities) identifies that standardised methodologies to characterise the flux footprint would be beneficial. In heterogeneous ice environments both ancillary data uncertainties and controls on gas exchange are notably complex. To address the poor understanding, we highlight how future efforts should focus on the collection of robust gas flux datasets within heterogeneous sea ice regions during key seasonal processes alongside consistent ancillary data with a full characterisation of their associated uncertainties.

1. Introduction

The ocean absorbs ~25% of all anthropogenic carbon dioxide (CO$_2$) emitted annually (Friedlingstein et al., 2020), mediating the impacts of anthropogenic climate change whilst driving ocean acidification (Clarke et al., 2017; Gao et al., 2012; Gattuso et al., 2015). Accurate estimates of this oceanic carbon sink are essential for balancing global and regional carbon budgets (Shutler et al., 2020) and carbon uptake in the polar oceans is an important component of the global oceanic total. The Arctic Ocean is estimated to be responsible for 5–15% of the total oceanic uptake (Bates and Mathis, 2009; MacGilchrist et al., 2014; Yasunaka et al., 2016) and the Southern Ocean for 40% (Caldeira and Duffy, 2000; Devries, 2014; Mikaloff Fletcher et al., 2006). However, large uncertainties in these polar estimates exist due to sparse polar measurements and the poorly understood influence of sea ice on air-sea gas exchange (Prytherch and Yelland, 2021).

Understanding the impact of sea ice on air-sea gas exchange is becoming increasingly important as the polar oceans respond to climate change. Strong Arctic amplification of global warming (Serreze and Barry, 2011) means Arctic sea ice is rapidly becoming thinner, with reduced coverage (Kwok and Rothrock, 2009; Kwok and Untersteiner, 2011; Meier et al., 2007; Serreze and Stroeve, 2015; Stroeve et al., 2012). As Arctic sea ice retreats, the width of the Arctic marginal ice zone (MIZ) is increasing (Strong and Rigor, 2013). In the Southern Ocean, climatic changes are modulating sea-ice extent (Parkinson, 2019), driving major shifts in the seasonality of sea ice (Stammerjohn et al., 2008) and an increase in storminess (e.g. Lubin et al., 2008). Storms amplify wave-ice interaction, with potential impacts on pancake ice formation, ice fragmentation and MIZ width (Massom and Stammerjohn, 2010). At both Poles, shifts in the sea-ice regime are influencing ice-ocean-atmosphere interactions and air-sea gas exchange.

The exchange of CO$_2$ across the air-water interface can occur in

---

* Corresponding author.
  E-mail address: j.h.watts@exeter.ac.uk (J. Watts).

either direction, depending on the air-sea concentration difference. Woolf et al. (2016) define the bulk air-sea gas flux as:

$$F_i = K_i(C_i - C_M), \tag{1}$$

where F_i is the vertical flux of CO_2 to/from the sea surface, K_i is the interfacial gas transfer velocity (herein referred to as K), C_i is the interfacial CO_2 concentration and C_M is the CO_2 concentration at the base of the ocean molecular boundary layer. The ocean molecular boundary layer is the thin layer at the ocean surface over which gradients of mass concentration associated with an air-sea disequilibrium are confined (Woolf et al., 2016). The CO_2 concentration is the product of the partial pressure of CO_2 ($\rho\, CO_2$) and solubility, which is predominantly temperature dependent (Woolf et al., 2016). K is the inverse of the resistance to gas transfer across the air-sea interface, and thus describes the efficiency of gas exchange (Liss and Slater, 1974). Air-sea CO_2 fluxes are influenced by factors that alter the air-sea concentration difference of CO_2 and/or K (Fig. 1). The bulk flux equation (Eq. (1)) is used to estimate net air-sea CO_2 fluxes scales (regional to global, daily to annual) required to constrain the global carbon budget. At present these are estimated to have a total global average uncertainty of $\pm 20\%$ (Woolf et al., 2019).

Uncertainty in K is considered to be the dominant source of uncertainty within global air-sea CO_2 flux estimates (Woolf et al., 2016). Wind speed is the primary physical force that drives near surface ocean turbulence and is thus the proxy used most often to parameterise open ocean K (Ho et al., 2011; Shutler et al., 2020; Wanninkhof, 2014). Existing parameterisations of K are typically empirically derived functions of horizontal wind speed at a height of 10 m (Wanninkhof, 2014; Lovely et al., 2015). However, there is evidence that a single wind speed parameterisation cannot adequately parameterise the gas transfer velocity for all oceanic conditions (Shutler et al., 2020; Wanninkhof et al., 2009). Specific examples from the literature are gas transfer velocity in estuarine/fjord environments (Banko-Kubis et al., 2019), conditions where wave breaking is driving bubble mediated gas transfer (Deike and Melville, 2018) or gas transfer velocity in the presence of surfactants (Pereira et al., 2018).

Wind speed-derived K in the sea-ice zone is often scaled to the fraction of open water (Stephens and Keeling, 2000; Arrigo and Van Dijken, 2007; Takahashi et al., 2009; Loose et al., 2014; Shutler et al., 2016). This assumes that all types of ice coverage at all times of year act as a complete barrier to gas exchange (Arrigo and Van Dijken, 2007; Stephens and Keeling, 2000; Takahashi et al., 2009), and that boundary layer dynamics in the open water portions of the icescape respond to wind forcing the same as in the open ocean. A simple linear scaling of K to sea ice concentration (SIC) offers a first approach, but has had limited evaluation in the field. Collated information from the literature on sea-ice processes relevant to gas exchange controls (Fig. 1) highlights that the relationship between sea ice and air-sea gas exchange controls is complex, particularly in mixed ice-water environments. Evidence has been presented that suggests sea ice, and ice-water interactions, can either inhibit (Bigdeli et al., 2018; Butterworth and Miller, 2016a; Prytherch et al., 2017; Rutgers Van Der Loeff et al., 2014) or enhance (Kohout and Meylan, 2008; Loose et al., 2017; McPhee and Martinson, 1994; Morison et al., 1992) gas exchange. The mismatch between practical applications of the impact of sea ice on gas exchange (e.g. the linear scaling method) and evidence from the literature drives a need for field-techniques that can make observations of gas exchange at scales compatible with improving K parameterisations for complex mixed ice-water environments.

Eddy covariance is a micrometeorological method used to quantify air-sea CO_2 fluxes using the covariance of rapid fluctuations in atmospheric gas concentrations and vertical wind velocities (Blomquist et al., 2014; Miller et al., 2010). K can be in-directly estimated from eddy covariance air-sea CO_2 flux datasets by rearranging the bulk flux equation (Eq. (1)) if solubility and CO_2 concentrations are also measured. Eddy covariance results are time-averaged (order of 20–180 min) and represent vertical fluxes from a 'source area' or 'flux footprint' upwind of the sensor (order of 100 m–1 km). It should also be noted that eddy covariance is not the only field technique for studying gas exchange processes in the presence of sea ice, there is also the radon-deficiency method (a mass balance method), which also provides an indirect estimate of K (e.g. Rutgers Van Der Loeff et al., 2014; Loose et al., 2017) and the enclosure method which has been used to measure gas fluxes through ice (e.g. Geilfus et al., 2014). While heterogeneous conditions present an inherent challenge (Bell et al., 2015; Hill et al., 2017) the ability of eddy covariance to capture data at temporal and spatial scales that encompass the natural heterogeneity of sea-ice and mixed ice-water
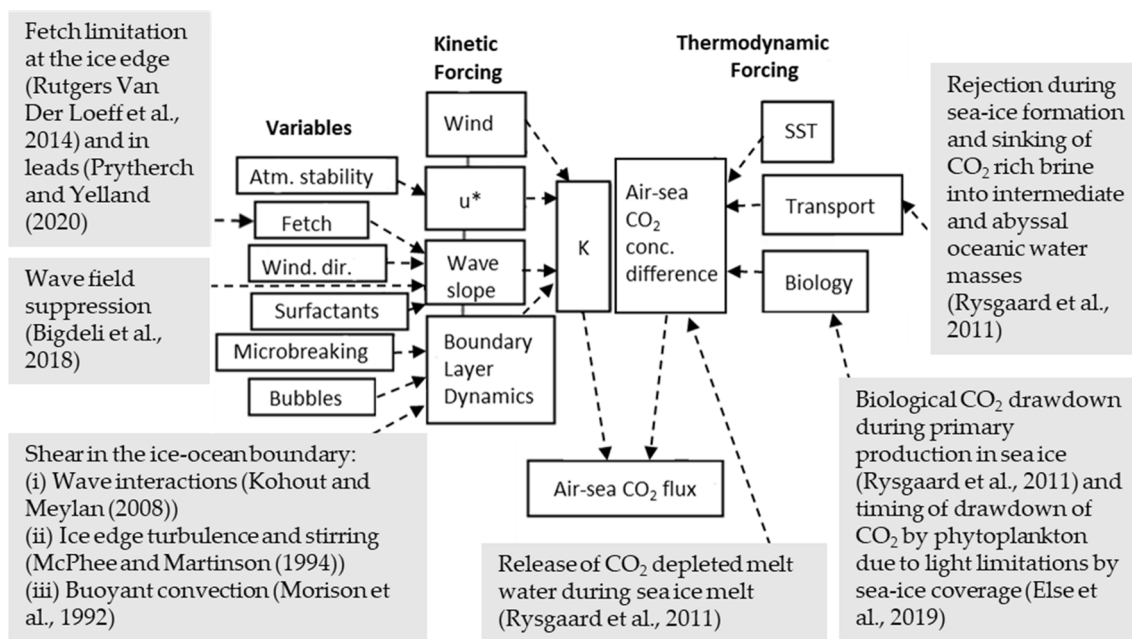

Fig. 1. Summary of air-sea gas exchange controls adapted from Wanninkhof et al. (2009) to include sea ice-relevant processes from the literature (grey shaded boxes).

environments is a major advantage over the enclosure (<1 m, >12 h) and radon-deficit methods (3–4 days, >10 km) (Butterworth and Else, 2018). The temporal and spatial scales of eddy covariance datasets means they can be used to study process-level variability in air-sea gas exchange, which in turn helps to determine which processes are relevant to estimates of regional to global air-sea fluxes made using the bulk flux equation (Eq. (1)). Improvements in eddy covariance methods that identify and reduce the uncertainties in these measurements are likely to increase the reconciliation between all the methodologies commonly used to study air-sea gas exchange, both fluxes and gas transfer velocity, and the oceanic carbon sink.

The eddy covariance technique has evolved considerably over the timeframe of the polar marine eddy covariance studies identified in this work (2004–2020) both as a result of the experimental set-up and post-processing techniques used to produce reliable measurements (see Dong et al., 2021a; Landwehr et al., 2015). To ascertain the current state of knowledge we present a critical review of the identified studies to address the following research questions:

1. **Can the results of historical polar eddy covariance studies of air-sea/air-ice-sea CO_2 fluxes be objectively compared?** We reviewed the study systems, methodologies and results of historical polar eddy covariance studies of CO_2 flux in regions of partial to full sea-ice coverage and placed their results in the context of recent advances in knowledge in the field.
2. **What are key sources of uncertainty in the interpretation of polar eddy covariance flux datasets?** Linked to the comparison of historical studies the review compared the usage, and associated uncertainties, of key ancillary datasets (e.g. air-sea concentration gradient of CO_2 and sea-ice data used for flux footprint characterisation).
3. **Where should future effort to understand polar air-sea gas exchange of CO_2 using eddy covariance be focussed?** Using the findings of the review process we identified focus areas for future studies.

2. Materials and methods

Papers that present air-sea fluxes of CO_2 in sea-ice environments measured using eddy covariance were collated using a literature search in Google Scholar. The search used the key terms 'eddy covariance', 'polar oceans', 'sea ice', 'CO_2 fluxes', 'gas fluxes', 'gas transfer velocity', 'air-sea gas fluxes', 'air-sea carbon-dioxide fluxes', 'air-sea gas exchange', 'Arctic', 'Antarctic', 'Southern Ocean'. Results were filtered to only include CO_2 fluxes measured using the eddy covariance technique in the Arctic or Southern Ocean in the presence of partial to full sea ice cover. The 'snowballing technique' was applied to identify any other relevant work, which uses the references of the papers identified in the search to identify further relevant titles for investigation (Creswell and Poth, 2016). Twelve papers were identified that met all the criteria.

3. Review of eddy covariance studies of air-sea exchange of CO_2 in sea-ice regions

Key information on the study system, experimental set-up and conclusions of the twelve identified polar eddy covariance studies is presented in Table 1. There are ten studies in the Arctic which include flux measurements made over landfast sea ice during spring melt season (Semiletov et al., 2004, 2007; Miller et al., 2011b; Papakyriakou and Miller, 2011; Butterworth and Else, 2018), over-winter in an active polynya (Else et al., 2011), in the Arctic MIZ through mid-summer to autumn (Prytherch et al., 2017) and over central Arctic Ocean pack-ice during summer (Prytherch and Yelland, 2021). In the Antarctic there are only two published studies, the first measured CO_2 fluxes over multiyear ice in the Weddell Sea (Zemmelink et al., 2006) and the second measured CO_2 fluxes over the Southern Ocean and Antarctic MIZ

through spring to summer (Butterworth and Miller, 2016b). Gas transfer velocity estimates are presented in three of these studies: Prytherch et al. (2017) in the Arctic MIZ; Butterworth and Miller (2016a) in the Antarctic MIZ; and Prytherch and Yelland (2021) over leads within central Arctic pack ice.

There are clear disparities in the study system, methodology and results of the identified studies (Table 1). Earlier studies have tended to conclude sea ice as an active component of the carbon cycle in a range of ice regimes. This includes observations of air-ice exchange over winter (Miller et al., 2011b), enhanced uptake over sea ice with melt ponds and through brine channels during spring melt season (Miller et al., 2011b; Papakyriakou and Miller, 2011; Semiletov et al., 2004, 2007) and enhanced exchange during active sea-ice formation (Else et al., 2011). Studies in both the Arctic MIZ (Prytherch et al., 2017) and Antarctic MIZ (Butterworth and Miller, 2016b) have presented evidence to suggest that it is reasonable to linearly scale K with SIC. Conversely, Prytherch & Yelland (2021) present evidence that K is supressed by 30% (compared to typical open-ocean parameterisations) within sea-ice leads. A table synthesising the full detailed methodology of each study is presented in supplementary materials (Table S1).

3.1. Closed-path gas analysers and sample drying

Eddy covariance requires high precision measurements of atmospheric CO_2 fluctuations. Open-path infrared gas analysers (IRGAs) produce unreliable results in marine environments due to biases driven by cross-sensitivities to water vapour (Blomquist et al., 2014; Kohsiek, 2000; Miller et al., 2010), which cannot be satisfactorily corrected for using post-hoc corrections (e.g. the WPL correction is too large for use in low flux environments (Jentzsch et al., 2021); and the PKT correction is ineffective (Landwehr et al., 2014)). This has significant consequences for earlier studies in which open-path gas analysers were used (see Table 1) prior to the identification of these instrument biases. The effect of open-path gas analysers is visible in these studies through the reporting of highly variable CO_2 fluxes in sea-ice regions, often including fluxes higher than typical open ocean values (Else et al., 2011; Miller et al., 2011b; Papakyriakou and Miller, 2011; Semiletov et al., 2007, 2004; Zemmelink et al., 2006). The lead authors of Else et al. (2011), Miller et al. (2011a) and Papakyriakou and Miller (2011) (L. Miller, T.Papkyriakou, personal communication via email, 11th September 2019) have confirmed that they do not consider the data produced in these studies to be as reliable as the measurements reported in more recent work.

More recent eddy covariance air/sea CO_2 flux measurements have made substantial progress through the use of closed path systems that eliminate water vapour fluctuations (Blomquist et al., 2014). Drying sample air substantially reduces the water vapour in the sample, removes the water vapour fluctuations and dramatically reduces the magnitude of associated corrections (Butterworth and Else, 2018; Miller et al., 2010; Webb et al., 1980). Comparison between dried and undried cavity ring down spectrometer (CRDS) flux measurements has also demonstrated that a numerical correction for mean water vapour content can be sufficient to yield accurate CO_2 fluxes when combined with a closed path setup (Yang et al., 2016). The authors demonstrated that a closed path system (i.e. sample air pulled through a length of tubing into the analyser) effectively eliminates the high frequency water vapour fluctuations that would otherwise affect the measured CO_2 flux. Closed path measurements made on dried air samples are presented in Sievers et al., (2015), Butterworth and Miller (2016a), Butterworth and Else (2018). Prytherch and Yelland (2021) used a closed path, Li-Cor with an undried sample but considered conditions to be sufficiently dry during the study period. Prytherch et al. (2017) used a closed path Los Gatos Research Fast Greenhouse Gas Analyser (a Cavity Ringdown Spectrometer) with an undried air sample and numerical water vapour correction. Gas transfer velocity estimates from closed path flux systems operated in open ocean environments now yield results that are typically

Table 1

Overview of polar air-sea CO_2 flux study sites and results. Shaded rows indicate when closed-path gas analysers were used.

Study	Platform/ location	Season/ ice conditions	Gas analyser	Findings/conclusions
Semiletov et al. (2004)	Land-based tower, Point Barrow, Arctic	Late Spring, Melting landfast ice	Not stated	Sea-ice melt ponds and open brine channels form an important CO_2 sink during spring/summer melt season.
Zemmelink et al. (2006)	Drift station on ice floe, Weddell Sea, Antarctica	Early summer, Multiyear ice	Open-path Li-Cor 7500	Uptake of CO_2 over snow covered multi-year sea ice of between -18.2 to -4.5 mmol m^{-2} d^{-1} driven by biological activity at the ice-snow interface.
Semiletov et al. (2007)	Land-based tower, Coastal zone of the Chukchi Sea	Mid-Spring, Melting landfast ice	Open-path Li-Cor 7500	Sea-ice melt ponds and open brine channel form important CO_2 sink during spring/summer melt season.
Else et al. (2011)	Ship-mounted, Arctic Polynya	Mid-winter, Active polynya	Open-path Li-Cor 7500	Enhanced air-sea gas exchange in mixed ice environments during ice formation.
Miller et al. (2011)	Land-based tower, Beaufort Sea	Winter to late Spring, Landfast ice (coldest period into spring melt)	Open-path Li-Cor 7500	Sea ice is an active participant in the carbon cycle.
Papakyriakou & Miller (2011)	Tower mounted on ice, Canadian Arctic Archipelago	Spring, Seasonal landfast ice	Open-path Li-Cor	High CO_2 fluxes (maximum efflux = 1, maximum uptake = -259.2 mmol m^{-2} d^{-1}) over seasonal landfast sea ice comparable with fluxes over land.

within 20% of other tracer-based estimates and can be used to investigate the small scale variability in K (Bell et al., 2017; Blomquist et al., 2017; Butterworth and Miller, 2016b; Dong et al., 2021b; Landwehr et al., 2018; Miller et al., 2009; Yang et al., 2021; Zavarsky et al., 2018).

3.2. Modelling the location of the flux footprint

The flux footprint position relative to the eddy covariance measurement location is determined by the wind direction, while footprint extent (distance from the measurement point that flux signals can be observed) is predominantly a function of measurement height as well as

Table 1 (*continued*)

			75 00	
Sørensen et al. (2014)	Tower mounted in ice, Greenland ic fjord	Late March, seasonal landfast ice	Open-path Li-Cor 7500	Air-ice fluxes between −244.5 to 86.4 mmol m^{-2} d^{-1}. Study proposes use of conceptual model for calculation of air–sea ice fluxes based on the resistance analogy
Sievers *et al.* (2015)	Ice mounted towers, Greenland ic fjord	Early March to late April, two landfast ice sites and a newly formed polynya	Open-path Li-Cor 7500	Outgassing (8.64 ±3 9.64 mmol m^{-2} day^{-1}) over one landfast ice site and uptake over the polynya (−9.9 7± 19.8 mmol m^{-2} day^{-1})
			Closed-path Li-Cor 7200	Outgassing (1.73 ± 5 mmol m^{-2} day^{-1}) with the progression of spring time warming and strong winds.
Butterworth & Miller (2016a)	Ship-mounted, Southern Ocean and Antarctic MIZ	Mid-summer through to early autumn, Antarctic MIZ	Closed-path Li-Cor 7200	Gas transfer velocity scales linearly with sea ice concentration in the MIZ.
Prytherch *et al.* (2017)	Ship-mounted, Arctic Ocean MIZ	Mid-summer to Autumn, Arctic MIZ	Los Gatos Fast Greenhouse Gas Analyser	Gas transfer velocity scales linearly with sea ice concentration in the MIZ.
Butterworth & Else (2018)	Land-based tower, Amunsden Gulf, Arctic	Spring to Summer, Landfast ice during Spring melt season	Closed-path Li-Cor 7200	Air-drying combined with closed path infrared gas analysers can reconcile eddy covariance and enclosure measured fluxes over landfast sea ice.
Prytherch & Yelland (2021)	Drift station on ice floe, Central Arctic Ocean	Late Summer to Early Autumn, Dense pack ice with lead systems	Closed-path Li-Cor 7200	Wind-speed dependent gas transfer velocity is supressed by 25-30% in leads relative to the open ocean.

aerodynamic surface roughness, horizontal wind speed and atmospheric stability (Kljun et al., 2015). The parameters required to estimate the flux footprint location and extent, can be determined from measurements made at the eddy covariance tower. However, it should be noted that sea ice characteristics (e.g. ice age, ice type, melt ponds, snow cover) will also impact the aerodynamic roughness length of sea ice (Andreas et al., 2010; Guest and Davidson, 1991; Smeets and Broeke, 2008; Weiss et al., 2011) and thus the flux footprint extent.

There has been limited evaluation of the spatial and temporal resolution of eddy covariance flux footprints in sea-ice regions and no comparison with the spatial resolution of concurrent sea ice and oceanic condition measurements. Of the studies in Table 1, only two studies present evidence of modelling the flux footprint. Butterworth and Else (2018) use the Kljun et al. (2015) flux footprint prediction model to exclude fluxes that had been influenced by land. Prytherch and Yelland (2021) evaluated the flux footprint estimation and its impact on the interpretation of their flux dataset. The authors used two models (Kljun et al. (2015); Hsieh et al. (2000)) to directly compare the CO_2 flux footprint with measurements of the lead dimensions. The relative proportions of water and ice in the footprint were determined with high precision using both models. Estimates of K were found to be sensitive to the model used to determine the open water fraction, however it was not possible to determine which footprint model is most accurate in regions with sea ice (Prytherch and Yelland, 2021). The Kljun et al. (2015) model is currently preferred due to its verification over a wider range of atmospheric conditions, and its lower sensitivity to small changes in atmospheric stability.

3.3. Characterisation of conditions in the flux footprint

The resolution of eddy covariance datasets means spatial measurements of sea ice and oceanic conditions within the air-sea gas flux footprint are required to understand the relationship between sea ice and measured CO_2 fluxes and/or inferred gas transfer velocities. Fixed point camera imagery, airborne imagery (e.g. from a helicopter) and satellite remote sensing data have all been used to provide spatial data to characterise sea ice during polar eddy covariance studies (see Table 2). However, not all of the studies identified in this work used spatial data to assess sea-ice conditions (e.g. Miller et al., 2011a; Papakyriakou and Miller, 2011; Sørensen et al., 2014; Sievers et al., 2015). Where spatial data has not been used, studies have tended to focus on air-ice-sea interactions and sea-ice has been characterised using vertical sea-ice properties (e.g. ice-depth, ice-temperature, ice-salinity, brine volume) and carbonate chemistry parameters (e.g. total inorganic carbon, total alkalinity). This type of data can only be collected within sea-ice environments where access by foot to collect ice cores is possible (e.g. landfast ice, large ice floes). Ultimately, this approach is limited in its ability to capture spatial heterogeneity at the scales relevant to the eddy covariance flux datasets.

To characterise ice conditions, Prytherch et al. (2017) and Butterworth and Else (2018) used Advanced Microwave Scanning Radiometer 2 (AMSR2) daily SIC derived using the ASI Arctic Radiation and Turbulence Interaction Study (Artist) Sea Ice algorithm (Spreen et al., 2008) at resolutions of 6.25 km and 3.125 km respectively. The Artist sea ice algorithm determines SIC from passive microwave observations, (see = Spreen et al. (2008) for further details). Both studies created concurrent time series of daily SIC coincident with measured air-sea gas fluxes, either for the grid-cell matched with the position of the vessel (Prytherch et al., 2017) or with the three grid cells closest to the eddy covariance tower (Butterworth and Else, 2018). Prytherch et al. (2017) also linearly interpolated SIC data to the 30-minute resolution flux measurement times.

Butterworth and Miller (2016a) determined SIC using fixed point camera images taken along-track at 1 Hz using digital cameras (CC5MPX; Campbell Scientific) mounted starboard and port on the RV Nathaniel B. Palmer ice-tower. Each image was orthorectified using

Table 2
Overview of polar eddy covariance air-sea gas flux study sea ice observation methodologies.

Study	Sea Ice Observation System	Spatial and Temporal Scale
Semiletov et al. (2004)	None.	N/A
Zemmelink et al. (2006)	Aerial Photography (visible light) and Electromagnetic soundings	70 km along either side of the floe
Semiletov et al. (2007)	None.	N/A
Else et al. (2011)	RADARSAT-1 ScanSAR (Synthetic Aperture Radar) narrow beam images.	50 m, as close to each case study as possible
Miller *et al.* (2011)	Ice and snow characteristics from ice cores. No spatial measurements of sea ice.	Discrete sampling, sub-daily
Papakyriakou and Miller (2011)	Sensors deployed in vicinity of EC equipment to measure snow and ice characteristics. No spatial measurements of sea ice.	Discrete sampling, sub-daily
Sørensen et al. (2014)	Ice and snow characteristics from ice cores. No spatial measurements of sea ice.	Discrete sampling, sub-daily
Sievers et al. (2015)	Ice and snow characteristics from ice cores. No spatial measurements of sea ice.	Discrete sampling, sub-daily
Butterworth and Miller (2016b)	Two mounted Campbell Scientific CC5MPX digital cameras	Image Footprint – 3000 m^2 (maximum width and length of trapezoid 55 m × 55 m). Photos taken every 1 s.
Prytherch et al. (2017)	Satellite Derived Passive Microwave SIC Data from AMSR2 using the Artist sea ice algorithm (ASI 5) (Spreen et al., 2008) interpolated to the flux measurement time.	6.25 km grid, daily
Butterworth and Else (2018)	Photos taken with a tower mounted (1) Go Pro Hero 4 and (2) Campbell Scientific CC5MPX digital camera, (3) Satellite Derived Passive Microwave SIC Data from AMSR2 using the Artist sea ice algorithm (ASI 5) (Spreen et al., 2008) (4) Landsat-8 and (5) MODIS images (5) Aerial photographs taken from a helicopter.	(1) unknown, hourly (2) unknown, every 5 min (3) 3.125 km grid (4) 30 m, every 8 days dependent on when cloud cover permits (5) 250 m, 1–2 days dependent on when cloud cover permits (6) variable
Prytherch, J. and Yelland, (2021)	Spatial dimensions of lead measured using a hand-held laser range finder (Naturalife PF4)	metres, attempted twice daily.

image coordinates obtained in a laboratory setting input into a geometric transformation script (imwarp.m) from MATLAB's image processing toolbox. To calculate SIC, the rectified images were converted to grayscale and a brightness threshold for ice manually assigned (Hall et al., 2002). Manual threshold assignment (not automated) was required due to variability in ice types, light conditions and glare. The percentage of ice pixels was then used to represent ice fraction (e.g. SIC). SIC was calculated in this way for one image every minute and averaged over 10 min to create a time-series of SIC concurrent with the gas flux dataset. Each image has a ~3000 m^2 footprint, which represents an area up to ~55 m in front of the vessel. The spatial resolution is thus directly related to the speed of the vessel. The spatial resolution of the extracted SIC data ranges from images with a footprint of ~3000 m^2 (i.e. ship's speed is zero) up to an area of horizontal distance of ~135,025 m^2 (maximum ship speed of 4 m s^{-1}). These back-of-the-envelope calculations highlight the potential for variability in the spatial resolution of data collected by fixed point camera systems on moving vessels. Bias, driven by natural variations in vessel speed in different ice and oceanic

conditions, will therefore need to be characterised in ship-mounted camera derived sea-ice datasets. In the eddy covariance flux studies shown in Table 1, methods to extract SIC from fixed point camera images have been relatively simple (e.g. Hall et al., 2002) and did not result in data with a clearly defined geographical extent. The spatial footprint of each image/image-set is ideally required for eddy covariance studies and should be determined using the field of view of the camera, mount height and viewing angle, camera location (coordinates), camera optics and, if from a moving platform, the speed of the vessel.

Measurement uncertainties associated with different sources of sea-

ice data are likely to impact polar air-sea gas flux data interpretation. Uncertainties in passive microwave measurements of SIC can occur when brightness temperature retrievals are affected by atmospheric absorption and emission uncertainties, in particular due to water vapour (Ivanova et al., 2015; Oelke, 1997), wind shear surface roughening effects (Andersen et al., 2006; Oelke, 1997), and smearing effects due to sharp concentration differences within the sensor footprint (Meier, 2005). Passive microwave uncertainties are inherently linked to mixed ice-water environments such as the MIZ, polynyas and the SIZ during autumn-freeze up and spring melt. In addition, wet surfaces (e.g. melt
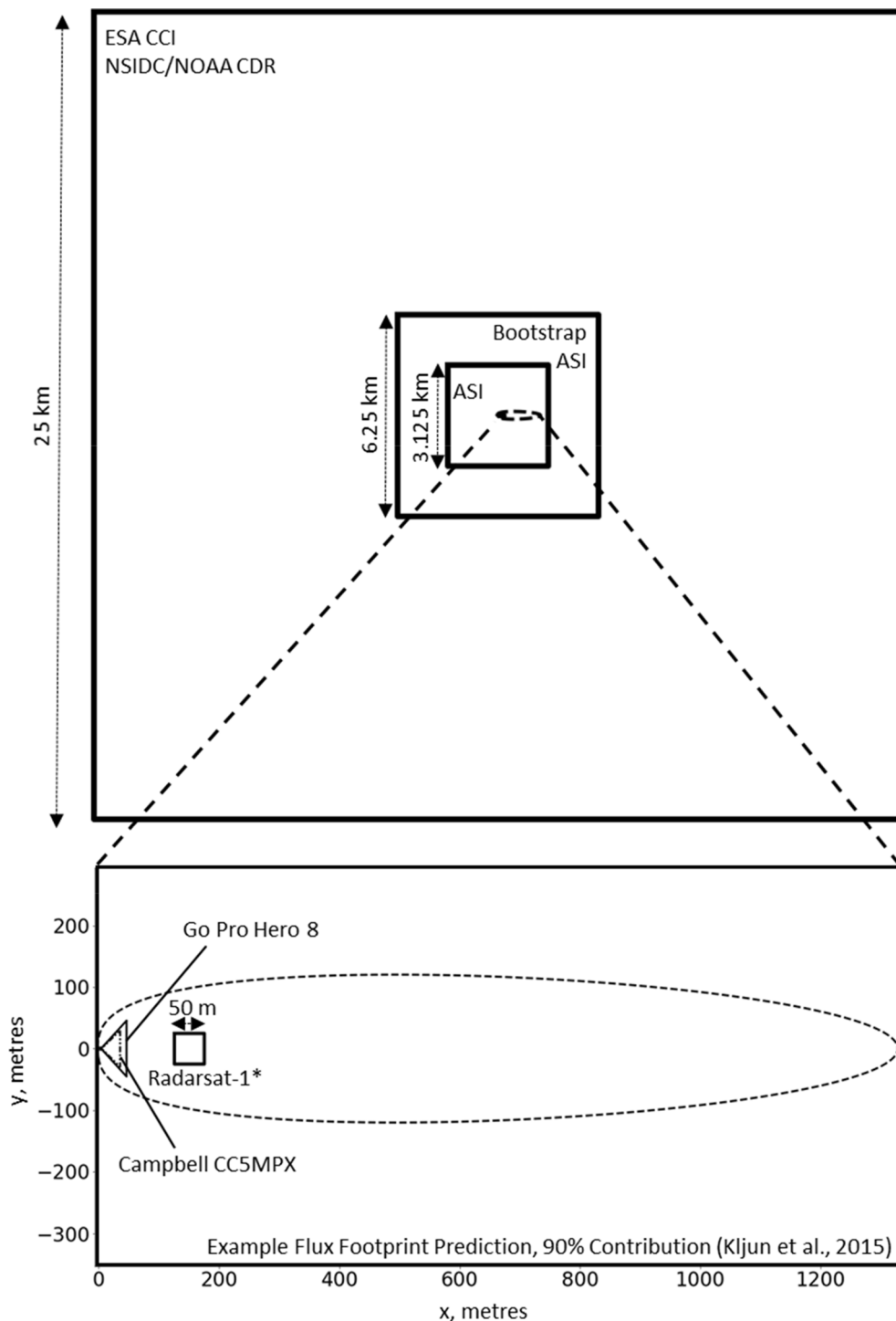

Fig. 2. Schematic comparing the footprint of *in situ* camera imaging (Campbell CC5MPX and Go Pro Hero 8, mounted at 12.5 m, angle = 45°) and the spatial resolution of typically available satellite data products (ESA CCI SIC (25 km) NSIDC/NOAA CDR SIC (25 km), AMSR2 ASI V5 SIC (3.125 km, 6.25 km), AMSR2 Bootstrap V5 SIC (6.25 km)) with example flux footprint model estimates (Kljun et al., 2015). The flux footprint model (90% contour line) is for a measurement height of 12.5 m, a roughness length (z_0) of 4.1×10^2 m (Antarctic pack ice, Weiss et al., 2011): a) frictional velocity (u_*) of 0.2, Obukhov length (L) of −50 m and boundary layer height (h) of 2500 m (following the convective scenario 10 in Table 2 of Kljun et al. (2015); b) u_* of 0.3, L of 200 m and h of 310 m (following stable scenario 16, Table 2, Kljun et al. 2015); c) represents the footprint for the stable scenario 17 with the same parameters as (b) but a measurement height of 15 m.

*Radarsat-1 data resolution, actual image footprints are 300 x 300 km

ponds) and thin sea-ice types (<0.15 m) cannot currently be accurately resolved (Ivanova et al., 2015; Massom, 2009; Meier, 2005). For example, Butterworth and Else (2018) observed that during spring melt season the AMSR2 passive microwave product underestimated SIC by up to 30%, when compared to *in situ* photographs, due to water on the ice surface. Uncertainties associated with SIC data obtained from ship-track or tower-based photos have received limited attention. Fixed point camera image uncertainties include pixel or 'perspective' distortion caused by oblique viewing angles, which causes warping or transformation of the image (Verykokou and Ioannidis, 2018; Zhang and Skjetne, 2018), radial distortion caused by non-rectilinear lenses (Zhang and Skjetne, 2018), and weather and sunlight conditions that influence contrast brightness (Gomez and Purdie, 2016; Kern et al., 2019). There is also potential for SIC differences between ship-based observations and satellite observations due to sampling bias. Ship observations are inherently biased toward low ice concentrations within heterogeneous ice fields because ships avoid thick and deformed sea ice (Kern et al., 2019).

The temporal and spatial resolution of sea-ice data may also impact comparison with eddy covariance flux observations. Eddy covariance datasets have a minimum temporal resolution on the order of 10 to 30 min and spatial resolution on the order of 100 m to 2 km (Dong, Yang, Bakker, Kitidis, *et al.*, 2021; Prytherch and Yelland, 2021). Direct comparison of the spatial resolutions of typically available satellite sea-ice data sources and fixed point camera image extent with flux footprints (e.g. as shown in Fig. 2) shows major discrepancies in their spatial extent and/or resolution. Mismatched resolutions between the flux data and footprint characterisation data are likely to be important, particularly in highly heterogeneous sea-ice environments. The RADARSAT-1 synthetic aperture radar (SAR) data used by Else et al. (2011) has a high spatial resolution (<50 m) compared to available passive microwave data (3.125–25 km) and can be used to determine not only ice concentration, but also ice type (e.g. Else et al., 2011, Park et al., 2019) and ice dynamics (Kozlov et al., 2020; Zhang et al., 2020). Grid-wise data on concentration and ice type extracted from SAR are not yet routinely available but are a promising option for future studies. Optical (visible light spectrum) remote sensing (e.g. Spreen and Kern, 2017) can provide high-spatial resolution imagery useful for many relevant sea ice parameters (e.g. ice concentration, ice type, melt pond fraction) but suffers from even greater temporal constraints due to cloud cover interference. Fixed point camera systems can provide high spatial resolution data, but the specifics vary due to the oblique viewing angle, and its impact on the final resolution of extracted parameters (e.g. SIC) has not been assessed.

Regarding temporal resolution, fixed point camera images can provide sub-daily to sub-hourly SIC as they are not limited by satellite orbit times. SAR data can provide data from which SIC can be extracted typically on a scale of 2–3 days, although this varies geographically and is dependent on the platform orbit and/or constellation. Conversely, passive microwave satellites provide a consistent daily SIC product. How these different resolutions impact results depends on the time-scale of variability of sea-ice conditions within the flux footprint (e.g. how quickly do sea ice conditions in the footprint vary and is this the same for all sea-ice environments?). Ice variability during stationary studies is dependent only on sea-ice processes (e.g. ice melt, ice motion, ice formation), while moving ship-based studies are dependent on ship speed and along-track regional differences in ice conditions (type, distribution). The impact of heterogeneous conditions are also inherently linked to the spatial (size and position) and temporal (variability in time) of the extent of the eddy covariance footprint. The footprint, where the measured gas flux is generated, effectively defines the physical 'area of interest' for interpreting the impact of air-ice-sea processes on measured gas fluxes.

Robust interpretations of gas transfer processes in the presence of sea ice require an evaluation of the suitability of flux footprint model input data. The usefulness of sea-ice data is dictated by its spatial and temporal resolutions and the length scale of variability of sea ice compared to the flux footprint extent. Only SIC data derived from passive microwave and fixed point-camera have been used to date to statistically assess sea-ice data and flux footprint analyses. A detailed analysis of the statisitical treatment of percentage sea ice versus eddy covariance flux datasets is needed to identify if results are sensitive to characteristics of the sea ice data used.

3.4. Inconsistent air-sea concentration difference measurements and calculations and their impact on gas transfer velocity calculations

Calculating K from eddy covariance datasets requires accurate field measurements of CO_2 on the water-side. (pCO_{2w}))) and the air-side (pCO_{2a}) of the interface (see Eq. (1)) (see Dong et al. (2021a) for an extensive discussion on the accuracy, precision and combined uncertainties associated with these measurements). Thermal and haline effects can significantly influence air-sea gas flux calculations due to their impact on CO_2 solubility, with the dominant effect caused by temperature (Woolf et al., 2016). Typical water sampling techniques (underway systems, niskin bottles) result in sub-surface measurements of pCO_{2w} that need to be corrected to be valid for the interfacial temperature. Vertical gradients occur due to both thermal stratification, which occurs mostly in the summer months due to increased solar radiation, and the 'cool skin effect', whereby the skin temperature (due to heat fluxes) is cooler than the underlying ocean. The impact of the vertical temperature gradients on the pCO_2 difference (ΔpCO_2) is likely to be of the order of 1 to 3 ppm (Woolf, D. personal communication, August 2020). The impact of this on the derived gas transfer will depend on the air-sea pCO_2 difference during each study. For example, the minimum ΔpCO_2 threshold in Prytherch et al. (2017) was 40 ppm, which implies a maximum possible error in the resulting K of ± 7.5% if these temperature gradient effects are ignored (i.e. 3/40 = 0.075). This effect should still be considered during the measurement process to minimise its impact, or the issue should be included within the uncertainty budget. Overall, reanalysis of eddy covariance datasets has shown that the impact of near-surface gradients can be anything from small to substantial (see Figure 3 in Holding et al. (2019) and so should be accounted for either wihin the uncertainty budget or quantified during fieldwork.

However, Freshwater inputs into the Arctic Ocean from rivers and sea-ice melt (Yamamoto-Kawai et al., 2009) result in widespread vertical stratification. Although salinity has a less significant impact on pCO_{2w} than temperature (Woolf et al., 2019) this haline stratification can result in vertical gradients in pCO_{2w} by suppressing mixing between layers. Field studies in the stratified Arctic found vertical gradients in pCO_{2w} at <7 m depth (Miller et al., 2019) and <2 m (Ahmed et al., 2020). Ultimately, these field studies suggest large (>15%) differences in regional (Ahmed et al., 2020) and basin-wide (Miller et al., 2019) flux estimates if sub-surface pCO_{2w} values are used. This effect is also illustrated in Dong et al. (2021b) who used eddy covariance flux measurements to infer that vertical pCO_{2w} gradients, driven predominantly by Arctic sea-ice melt water, could lead to a 6%–17% underestimate of the annual Arctic Ocean CO_2 uptake. Dong et al (2021b) found that if unidentified these gradients in pCO_{2w} can significantly bias the eddy covariance derived K.

In regions with haline stratification differences in pCO_{2w} due to variable measurement depth and water sampling methodology cannot easily be corrected in post-processing, although some authors have tried (e.g Ahmed et al. (2020)). Post-processing will be complex and highly uncertain, particularly where multiple processes drive the stratification (Miller et al., 2019). Horizontal variability in pCO_{2w} may also be a concern over the spatial scales commonly captured within a flux footprint. During spring and summer, ice floes that are actively melting can cause plumes of low salinity (and typically low pCO_{2w}) surface water (e. g. Else et al., 2012). Under certain conditions (particularly light winds and low wave state), these plumes could create horizontal gradients on the scale of meters to kilometres that may result in significant pCO_{2w}

variability across a flux footprint. Similar issues likely arise during freeze-up, where frazil ice is produced in open water portions of the icescape and then advected horizontally to eventually accrete on the edges of floes (Else et al., 2011). These dynamic processes suggest that a single pCO_{2w} measurement within a flux footprint may not be sufficient to fully characterize the area of interest.

The method of pCO_{2w} measurement method and depth varies in the studies reviewed here (Table 1). For measurements made by the ship's underway system the depths of intake have differed between ~5 m (Else et al., 2011; Butterworth and Miller, 2016a) to ~8 m (Prytherch et al., 2017), as well as rosette samples collected at 5 and 10 m and interpolated (in time and space) to the flux measurement periods (Prytherch et al., 2017). Overall, pCO_{2w} corrections for vertical temperature gradients, the cool skin effect, and differences in water sampling technique are not discussed in any of the studies.

To reduce uncertainties in estimates of K, measurements of pCO_{2w} must be corrected for vertical gradients in temperature (cool skin effect, thermal stratification) in order to represent the surface layer pCO_{2w}. To reduce uncertainty, water samples should be made as close to the surface as possible, or at least verified as being made within the top mixed layer of the ocean. Sampling should ideally be conducted away from large ships to reduce disturbance (Yasunaka et al., 2018), which is challenging when the underway system is the most consistent method of obtaining high temporal and spatial resolution pCO_{2w}. Ideally, several pCO_{2w} measurements would be made across the flux footprint to characterize horizontal gradients. Access to undisturbed pCO_{2w} in surface waters between ice floes is an additional sampling challenge and source of uncertainty. Underway systems are often shut off in brash ice environments to prevent damage to the system and accessing surface waters between floes using other water sampling methodologies (e.g. niskin bottles) is challenging. Ancillary data on the vertical structure (undisturbed by the vessel itself) of the water column (temperature and salinity) and its variability in time and space within the flux footprint should be collected, particularly in physically complex environments (e.g. stratified coastal Arctic waters).

4. Conclusions and recommendations

This work presents an overview and critical review of the findings and methodologies of polar air-sea CO_2 eddy covariance field studies, with a specific focus on gas transfer velocity. There are currently only five studies that present best-practice (closed-path gas analyser, dried or otherwise corrected for humidity bias - see Section 3.1.1) eddy covariance measurements of air-ice-sea CO_2 fluxes and/or air-sea CO_2 fluxes in the presence of sea ice. And three of these studies present estimates of gas transfer velocity in mixed ice-water environments. Clearly conducting eddy covariance field studies in polar regions is challenging due to the harsh and remote environment. But this review highlights that there is a lack of reliable eddy covariance flux measurements over Antarctic multi-year ice (Zemmelink et al., 2006) and active polynyas (Else et al., 2011) and no eddy covariance studies of gas transfer velocity during key seasonal processes such as spring-melt season, early ice break up and sea-ice formation. There is a substantial knowledge gap concerning gas exchange in regions of partial to full sea ice coverage, and uncertainties remain greatest in heterogeneous mixed-ice water environments with intermediate SIC. Air-sea gas exchange is uncertain in regions of intermediate ice coverage where observations of the gas transfer velocity are either highly variable or poorly constrained (Fanning and Torres, 1991; Loose et al., 2017; Rutgers Van Der Loeff et al., 2014). Future efforts to understand polar air-sea gas exchange of CO_2 using eddy covariance should be focussed in these environments to improve understanding of whether current sea-ice zone parameterisations of gas transfer are appropriate for use in regional and global air-sea CO_2 flux estimates (research question 3).

Using eddy covariance air-sea CO_2 flux datasets to study the relationship between gas exchange and sea ice requires ancillary data on

sea-ice conditions in the air-sea flux footprint. Each of the five highlighted studies in Table 1 has taken a different approach to characterising sea-ice conditions concurrent with measured fluxes. Within this, the impact of using different resolution sea-ice datasets on findings has not been assessed. The spatial and temporal scales of sea-ice data and the flux footprint appear mismatched and the impact of this on flux dataset interpretation remains unexamined.

The ice characterisation in the studies in which the gas transfer velocity is calculated focus largely on SIC. It is likely that the broader impacts of sea ice and ice-water dynamics on gas exchange will need to be considered in order to reconcile theory with field measurements. We recommend that characteristics of the sea ice environment other than SIC are included in future field studies, as supported by Loose et al., (2014) and the findings of Prytherch and Yelland (2021). These could include, but are not limited to: ice type, ice thickness, lead dimensions, ice-water interactions (e.g. ice motion, ice edge stirring), floe size distribution, melt ponds and sea surface roughness.

This review has also highlighted that previous studies used different water sampling techniques at different water depths and without consideration of vertical temperature gradients when calculating the air-sea concentration difference. In addition, any reconciliation of results is further complicated due to incomplete and/or uncalculated uncertainty components that are likely influencing the high variability within any measured fluxes in sea-ice environments.

Overall, without calculated uncertainty components the observed differences in study system and methodology mean the results of historical polar eddy covariance studies of air-sea/air-ice-sea CO_2 fluxes are difficult to objectively compare (research question 1). Key sources of uncertainty in the interpretation of polar eddy covariance flux datasets are identified as: i) the gas analysis technique used, ii) water sampling methodology, iii) corrections for vertical gradients in pCO_{2w}, and iv) the spatial and temporal resolution of data used to characterise the air-sea flux footprint (research question 2).

To reconcile these issues, observations need to be comparable using a standardised methodology along with more complete uncertainty assessments. This should build on the uncertainty assessment made by Dong et al., 2021a in marine environments, which covers uncertainties not discussed in this work (e.g. ship motion, airflow distortion, inlet effects, spatial separation between the anemometer and inlet, sensor calibration and propagated bias). In the open ocean, Dong et al. (2021a) conclude that relative uncertainty in EC CO_2 fluxes is 20–50%, with greater uncertainty when CO_2 fluxes are small. The flux uncertainty can be reduced by averaging for longer (up to 3 hrs), with the required averaging period inversely related to the magnitude of ΔCO_2 The application of a standardised methodology with characterised uncertainties would make it possible to create an inventory of comparable eddy covariance CO_2 flux datasets. Studies can make use of remotely sensed data to characterise conditions within the flux footprint, and the uncertainty of the remote sensing data should be incorporated into the analysis in order to closely examine the process-level controls on air-sea gas exchange in the presence of sea ice. As a starting point for developing a 'best-practice' methodology, we recommend the following:

1. Only closed-path gas analysis techniques (either closed-path or cavity ring down gas analysers), with appropriate air-drying and/or water vapour corrections should be used.
2. The length scales of variability of the flux footprint and sea ice compared to the resolution of data characterising the footprint (whether satellite or fixed point-camera) should be characterised. This would need to characterise the full range of environments/ice-water conditions occurring throughout any gas flux data measurement period (as conditions will likely change).
3. Focusing on characterising sea-ice coverage within the modelled flux footprint e.g. build upon the workflow presented in Prytherch and Yelland (2021).

4. For the application of fixed-point cameras, additional work is needed to determine: (i) if the spatial resolution and resultant re-projection of aerial imagery from a fixed-point camera is adequate to characterise conditions within the flux footprint; and (ii) a best practice and consistent method for camera installation and data processing.

5. Water sampling recommendations made in Miller et al. (2019) should be followed (i.e. samples collected using a consistent technique and as close to the surface as possible).

6. Air-sea CO_2 concentrations should account for vertical temperature gradients, including the cool skin effect as identified in Watson et al. (2020).

7. Collection of ancillary data on pCO_{2w} gradients and water column structure, particularly away from the vessel if an underway system is being used, is recommended to aid interpretation of results

Declaration of Competing Interest

The authors declare that they have no known competing financial interests or personal relationships that could have appeared to influence the work reported in this paper.

Acknowledgments

Appendix A. Supplementary data

Supplementary data to this article can be found online at https://doi.org/10.1016/j.pocean.2022.102741.

References

Ahmed, M.M.M., Else, B.G.T., Capelle, D., Miller, L.A., Papakyriakou, T., 2020. Underestimation of surface p CO 2 and air-sea CO 2 fluxes due to freshwater stratification in an Arctic shelf sea. Hudson Bay. Elem. Sci. Anthr. 8 https://doi.org/10.1525/elementa.084.

Andersen, S., Tonboe, R., Kern, S., Schyberg, H., 2006. Improved retrieval of sea ice total concentration from spaceborne passive microwave observations using numerical weather prediction model fields: An intercomparison of nine algorithms. Remote Sens. Environ. 104 (4), 374–392. https://doi.org/10.1016/j.rse.2006.05.013.

Andreas, E.L., Horst, T.W., Grachev, A.A., Persson, P.O.G., Fairall, C.W., Guest, P.S., Jordan, R.E., 2010. Parametrizing turbulent exchange over summer sea ice and the marginal ice zone. Q. J. R. Meteorol. Soc. 136 (649), 927–943. https://doi.org/10.1002/qj.618.

Arrigo, K.R., Van Dijken, G.L., 2007. Interannual variation in air-sea CO 2 flux in the Ross Sea, Antarctica: A model analysis. J. Geophys. Res. Ocean. 112, C03020. https://doi.org/10.1029/2006JC003492.

Banko-Kubis, H.M., Wurl, O., Mustaffa, N.I.H., Ribas-Ribas, M., 2019. Gas transfer velocities in Norwegian fjords and the adjacent North Atlantic waters. Oceanologia 61 (4), 460–470. https://doi.org/10.1016/j.oceano.2019.04.002.

Bates, N.R., Mathis, J.T., 2009. The Arctic Ocean marine carbon cycle: Evaluation of air-sea CO 2 exchanges, ocean acidification impacts and potential feedbacks. Biogeosciences 6, 2433–2459. https://doi.org/10.5194/bg-6-2433-2009.

Bell, T.G., De Bruyn, W., Marandino, C.A., Miller, S.D., Law, C.S., Smith, M.J., Saltzman, E.S., 2015. Dimethylsulfide gas transfer coefficients from algal blooms in the Southern Ocean 15, 1783–1794. Doi: 10.5194/acp-15-1783-2015.

Bell, T.G., Landwehr, S., Miller, S.D., De Bruyn, W.J., Callaghan, A.H., Scanlon, B., Ward, B., Yang, M., Saltzman, E.S., 2017. Estimation of bubble-mediated air-sea gas exchange from concurrent DMS and CO 2 transfer velocities at intermediate-high wind speeds. Atmos. Chem. Phys. 17, 9019–9033. https://doi.org/10.5194/acp-17-9019-2017.

Bigdeli, A., Hara, T., Loose, B., Nguyen, A.T., 2018. Wave Attenuation and Gas Exchange Velocity in Marginal Sea Ice Zone. J. Geophys. Res. Ocean. 123 (3), 2293–2304. https://doi.org/10.1002/2017JC013380.

Blomquist, B.W., Brumer, S.E., Fairall, C.W., Huebert, B.J., Zappa, C.J., Brooks, I.M., Yang, M., Bariteau, L., Prytherch, J., Hare, J.E., Czerski, H., Matei, A., Pascal, R.W., 2017. Wind Speed and Sea State Dependencies of Air-Sea Gas Transfer: Results From the High Wind Speed Gas Exchange Study (HiWinGS). J. Geophys. Res. Ocean. 122 (10), 8034–8062. https://doi.org/10.1002/2017JC013181.

Blomquist, B.W., Huebert, B.J., Fairall, C.W., Bariteau, L., Edson, J.B., Hare, J.E., McGillis, W.R., 2014. Advances in Air-Sea CO 2 Flux Measurement by Eddy

Correlation. Boundary-Layer Meteorol. 152, 245–276. https://doi.org/10.1007/s10546-014-9926-2.

Butterworth, B.J., Else, B.G.T., 2018. Dried, closed-path eddy covariance method for measuring carbon dioxide flux over sea ice. Atmos. Meas. Tech. 11 (11), 6075–6090. https://doi.org/10.5194/amt-11-6075-201810.5194/amt-11-6075-2018-supplement.

Butterworth, B.J., Miller, S.D., 2016a. Automated underway eddy covariance system for air-sea momentum, heat, and CO 2 fluxes in the Southern Ocean. J. Atmos. Ocean. Technol. 33, 635–652. https://doi.org/10.1175/JTECH-D-15-0156.1.

Butterworth, B.J., Miller, S.D., 2016b. Air-sea exchange of carbon dioxide in the Southern Ocean and Antarctic marginal ice zone. Geophys. Res. Lett. 43 (13), 7223–7230. https://doi.org/10.1002/2016GL069581.

Caldeira, K., Duffy, P.B., 2000. The role of the southern ocean in uptake and storage of anthropogenic carbon dioxide. Science (80-) 287 (5453), 620–622.

Clarke, J.S., Achterberg, E.P., Connelly, D.P., Schuster, U., Mowlem, M., 2017. Developments in marine pCO 2 measurement technology; towards sustained in situ observations. TrAC Trends in Analytical Chemistry 88, 53–61. https://doi.org/10.1016/j.trac.2016.12.008.

Creswell, J.W., Poth, C.N., 2016. Qualitative Inquiry & Research Design: Choosing among Five Approaches. Sage Publications, Los Angeles, CA.

Deike, L., Melville, W.K., 2018. Gas Transfer by Breaking Waves. Geophys. Res. Lett. 45 (19), 10,482–10,492. https://doi.org/10.1029/2018GL078758.

DeVries, T., 2014. The oceanic anthropogenic CO 2 sink: Storage, air-sea fluxes, and transports over the industrial era. Global Biogeochem. Cycles 28 (7), 631–647. https://doi.org/10.1002/2013GB004739.

Dong, Y., Yang, M., Bakker, D., Kitidis, V., Bell, T., 2021a. Uncertainties in eddy covariance air-sea CO 2 flux measurements and implications for gas transfer velocity parameterisations. Atmos. Chem. Phys. 1–43 https://doi.org/10.5194/acp-2021-120.

Dong, Y., Yang, M., Bakker, D.C.E., Liss, P.S., Kitidis, V., Brown, I., Chierici, M., Fransson, A., Bell, T.G., 2021b. Near-surface Stratification Due to Ice Melt Biases Arctic Air-Sea CO 2 Flux Estimates. Geophys. Res. Lett. 48 (22) https://doi.org/10.1029/2021GL095266.

Else, B., Galley, R., Papakyriakou, T.N., Miller, L., Mucci, A., Barber, D., 2012. Sea Surface pCO 2 cycles and CO 2 fluxes at landfast sea ice edges in Amundsen Gulf, Canada. Journal of Geophysical Research 117. https://doi.org/10.1029/2012JC007901.

Else, B.G.T., Papakyriakou, T.N., Galley, R.J., Drennan, W.M., Miller, L.A., Thomas, H., 2011. Wintertime CO 2 fluxes in an Arctic polynya using eddy covariance: Evidence for enhanced air-sea gas transfer during ice formation. J. Geophys. Res. Ocean. 116 https://doi.org/10.1029/2010JC006760.

Fanning, K.A., Torres, L.M., 1991. 222 Rn and 226 Ra: indicators of sea-ice effects on air-sea gas exchange. Polar Res. 10 (1), 51–58. https://doi.org/10.3402/polar.v10i1.6727.

Friedlingstein, P., O'Sullivan, M., Jones, M.W., Andrew, R.M., Hauck, J., Olsen, A., Peters, G.P., Peters, W., Pongratz, J., Sitch, S., Le Quéré, C., Canadell, J.G., Ciais, P., Jackson, R.B., Alin, S., Aragão, L.E.O.C., Arneth, A., Arora, V., Bates, N.R., Becker, M., Benoit-Cattin, A., Bittig, H.C., Bopp, L., Bultan, S., Chandra, N., Chevallier, F., Chini, L.P., Evans, W., Florentie, L., Forster, P.M., Gasser, T., Gehlen, M., Gilfillan, D., Gkritzalis, T., Gregor, L., Gruber, N., Harris, I., Hartung, K., Haverd, V., Houghton, R.A., Ilyina, T., Jain, A.K., Joetzjer, E., Kadono, K., Kato, E., Kitidis, V., Korsbakken, J.I., Landschützer, P., Lefèvre, N., Lenton, A., Lienert, S., Liu, Z., Lombardozzi, D., Marland, G., Metzl, N., Munro, D.R., Nabel, J.E.M.S., Nakaoka, S.-I., Niwa, Y., O'Brien, K., Ono, T., Palmer, P.I., Pierrot, D., Poulter, B., Resplandy, L., Robertson, E., Rödenbeck, C., Schwinger, J., Séférian, R., Skjelvan, I., Smith, A.J.P., Sutton, A.J., Tanhua, T., Tans, P.P., Tian, H., Tilbrook, B., van der Werf, G., Vuichard, N., Walker, A.P., Wanninkhof, R., Watson, A.J., Willis, D., Wiltshire, A.J., Yuan, W., Yue, X.u., Zaehle, S., 2020. Global Carbon Budget 2020. Earth Syst. Sci. Data 12 (4), 3269–3340. https://doi.org/10.5194/essd-12-3269-202010.5194/essd-12-3269-2020-supplement.

Gao, K., Helbling, E.W., Häder, D.P., Hutchins, D.A., 2012. Responses of marine primary producers to interactions between ocean acidification, solar radiation, and warming. Mar. Ecol. Prog. Ser. 470, 167–189. https://doi.org/10.3354/meps10043.

Gattuso, J.P., Magnan, A., Billé, R., Cheung, W.W.L., Howes, E.L., Joos, F., Allemand, D., Bopp, L., Cooley, S.R., Eakin, C.M., Hoegh-Guldberg, O., Kelly, R.P., Pörtner, H.O., Rogers, A.D., Baxter, J.M., Laffoley, D., Osborn, D., Rankovic, A., Rochette, J., Sumaila, U.R., Treyer, S., Turley, C., 2015. Contrasting futures for ocean and society from different anthropogenic CO 2 emissions scenarios. Science 80-. https://doi.org/10.1126/science.aac4722.

Geilfus, N.X., Tison, J.L., Ackley, S.F., Galley, R.J., Rysgaard, S., Miller, L.A., Delille, B., 2014. Sea ice pCO 2 dynamics and air-ice CO 2 fluxes during the sea ice mass balance in the Antarctic (SIMBA) experiment – Bellingshausen sea. Antarctica Cryosphere 8, 2395–2407. https://doi.org/10.5194/tc-8-2395-2014.

Gomez, C., Purdie, H., 2016. UAV- based Photogrammetry and Geocomputing for Hazards and Disaster Risk Monitoring – A Review. Geoenvironmental Disasters 3 (1). https://doi.org/10.1186/s40677-016-0060-y.

Guest, P.S., Davidson, K.L., 1991. The aerodynamic roughness of different types of sea ice. J. Geophys. Res. 96, 4709–4721. https://doi.org/10.1029/90JC02261.

Hall, R., Hughes, N., Wadhams, P., 2002. A systematic method of obtaining ice concetration measurements from ship-based observations. Cold Regions Science and Technology 34, 97–102. https://doi.org/10.1016/S0165-232X(01)00057-X.

Hill, T., Chocholek, M., Clement, R., 2017. The case for increasing the statistical power of eddy covariance ecosystem studies: why, where and how? Glob. Chang. Biol. 23 (6), 2154–2165. https://doi.org/10.1111/gcb.13547.

Ho, D.T., Wanninkhof, R., Schlosser, P., Ullman, D.S., Hebert, D., Sullivan, K.F., 2011. Toward a universal relationship between wind speed and gas exchange: Gas transfer

velocities measured with 3He/SF6 during the Southern Ocean Gas Exchange Experiment. J. Geophys. Res. Ocean. 116 https://doi.org/10.1029/2010JC006854.

Holding, T., Ashton, I.G., Shutler, J.D., Land, P.E., Nightingale, P.D., Rees, A.P., Brown, I., Piolle, J.F., Kock, A., Bange, H.W., Woolf, D.K., Goddijn-Murphy, L., Pereira, R., Paul, F., Girard-Ardhuin, F., Chapron, B., Rehder, G., Ardhuin, F., Donlon, C.J., 2019. The fluxengine air-sea gas flux toolbox: Simplified interface and extensions for in situ analyses and multiple sparingly soluble gases. Ocean Sci. 15, 1707–1728. https://doi.org/10.5194/os-15-1707-2019.

Hsieh, C.-I., Katul, G., Chi, T.-W., 2000. An approximate analytical model for footprint estimation of scalar fluxes in thermally stratified atmospheric flows. Adv. Water Resour. 23 (7), 765–772. https://doi.org/10.1016/S0309-1708(99)00042-1.

Ivanova, N., Pedersen, L.T., Tonboe, R.T., Kern, S., Heygster, G., Lavergne, T., Sørensen, A., Saldo, R., Dybkjær, G., Brucker, L., Shokr, M., 2015. Inter-comparison and evaluation of sea ice algorithms: Towards further identification of challenges and optimal approach using passive microwave observations. Cryosphere 9, 1797–1817. https://doi.org/10.5194/tc-9-1797-2015.

Jentzsch, K., Boike, J., Foken, T., 2021. Importance of the WPL correction for the measurement of small CO_2 fluxes. Atmos. Meas. Tech. Discuss. 1–10 https://doi.org/10.5194/amt-2021-249.

Kern, S., Lavergne, T., Notz, D., Toudal Pedersen, L., Tage Tonboe, R., Saldo, R., Macdonald Sørensen, A., 2019. Satellite passive microwave sea-ice concentration data set intercomparison: Closed ice and ship-based observations. Cryosphere 13, 3261–3307. https://doi.org/10.5194/tc-13-3261-2019.

Kljun, N., Calanca, P., Rotach, M.W., Schmid, H.P., 2015. A simple two-dimensional parameterisation for Flux Footprint Prediction (FFP). Geosci. Model Dev. 8, 3695–3713. https://doi.org/10.5194/gmd-8-3695-2015.

Kohout, A.L., Meylan, M.H., 2008. An elastic plate model for wave attenuation and ice floe breaking in the marginal ice zone. J. Geophys. Res. 113, C09016. https://doi.org/10.1029/2007JC004434.

Kohsiek, W., 2000. Water Vapor Cross-Sensitivity of Open Path H_2O/CO_2 Sensors. J. Atmos. Ocean. Technol. 17, 299–311. https://doi.org/10.1175/1520-0426(2000)017<0299:WVCSOO>2.0.CO;2.

Kozlov, I.E., Plotnikov, E.V., Manucharyan, G.E., 2020. Brief Communication: Mesoscale and submesoscale dynamics in the marginal ice zone from sequential synthetic aperture radar observations. Cryosphere 14, 2941–2947. https://doi.org/10.5194/tc-14-2941-2020.

Kwok, R., Rothrock, D.A., 2009. Decline in Arctic sea ice thickness from submarine and ICESat records: 1958-2008: ARCTIC SEA ICE THICKNESS. Geophys. Res. Lett. 36 (15), n/a–n/a.

Kwok, R., Untersteiner, N., 2011. The thinning of Arctic sea ice. Phys. Today 64 (4), 36–41. https://doi.org/10.1063/1.3580491.

Landwehr, S., Miller, S.D., Smith, M.J., Bell, T.G., Saltzman, E.S., Ward, B., 2018. Using eddy covariance to measure the dependence of air-sea CO_2 exchange rate on friction velocity. Atmos. Chem. Phys. 18, 4297–4315. https://doi.org/10.5194/acp-18-4297-2018.

Landwehr, S., Miller, S.D., Smith, M.J., Saltzman, E.S., Ward, B., 2014. Analysis of the PKT correction for direct CO_2 flux measurements over the ocean. Atmos. Chem. Phys. 14, 3361–3372. https://doi.org/10.5194/acp-14-3361-2014.

Landwehr, S., O'Sullivan, N., Ward, B., 2015. Direct flux measurements from mobile platforms at sea: Motion and airflow distortion corrections revisited. J. Atmos. Ocean. Technol. 32, 1163–1178. https://doi.org/10.1175/JTECH-D-14-00137.1.

Liss, P.S., Slater, P.G., 1974. Flux of gases across the Air-Sea interface. Nature 247 (5438), 181–184. https://doi.org/10.1038/247181a0.

Loose, B., Kelly, R.P., Bigdeli, A., Williams, W., Krishfield, R., Rutgers van der Loeff, M., Moran, S.B., 2017. How well does wind speed predict air-sea gas transfer in the sea ice zone? A synthesis of radon deficit profiles in the upper water column of the Arctic Ocean. J. Geophys. Res. Ocean. 122 (5), 3696–3714. https://doi.org/10.1002/2016JC012460.

Loose, B., McGillis, W.R., Perovich, D., Zappa, C.J., Schlosser, P., 2014. A parameter model of gas exchange for the seasonal sea ice zone. Ocean Sci. 10 (1), 17–28. https://doi.org/10.5194/os-10-17-201410.5194/os-10-17-2014-supplement.

Lovely, A., Loose, B., Schlosser, P., McGillis, W., Zappa, C., Perovich, D., Brown, S., Morell, T., Hsueh, D., Friedrich, R., 2015. The Gas Transfer through Polar Sea ice experiment: Insights into the rates and pathways that determine geochemical fluxes. J. Geophys. Res. Ocean. 120, 8177–8194. https://doi.org/10.1002/2014JC010607.

Lubin, D., Wittenmyer, R.A., Bromwich, D.H., Marshall, G.J., 2008. Antarctic Peninsula mesoscale cyclone variability and climatic impacts influenced by the SAM. Geophys. Res. Lett. 35, L02808. https://doi.org/10.1029/2007GL032170.

MacGilchrist, G.A., Naveira Garabato, A.C., Tsubouchi, T., Bacon, S., Torres-Valdés, S., Azetsu-Scott, K., 2014. The Arctic Ocean carbon sink. Deep. Res. Part I Oceanogr. Res. Pap. 86, 39–55. https://doi.org/10.1016/j.dsr.2014.01.002.

Massom, R.A., 2009. Principal uses of remote sensing in a sea ice field research. F. Tech. Sea Ice Res. 405–466.

Massom, R.A., Stammerjohn, S.E., 2010. Antarctic sea ice change and variability - Physical and ecological implications. Polar Sci. 4 (2), 149–186. https://doi.org/10.1016/j.polar.2010.05.001.

McPhee, M.G., Martinson, D.G., 1994. Turbulent mixing under drifting pack ice in the Weddell Sea. Science (80-. 263 (5144), 218–221.

Meier, W.N., 2005. Comparison of passive microwave ice concentration algorithm retrievals with AVHRR imagery in arctic peripheral seas. IEEE Trans. Geosci. Remote Sens. 43 (6), 1324–1337. https://doi.org/10.1109/TGRS.2005.846151.

Meier, W.N., Stroeve, J., Fetterer, F., 2007. Whither Arctic sea ice? A clear signal of decline regionally, seasonally and extending beyond the satellite record. In: Annals of Glaciology. pp. 428–434. Doi: 10.3189/172756407782871170.

Mikaloff Fletcher, S.E., Gruber, N., Jacobson, A.R., Doney, S.C., Dutkiewicz, S., Gerber, M., Follows, M., Joos, F., Lindsay, K., Menemenlis, D., Mouchet, A.,

Müller, S.A., Sarmiento, J.L., 2006. Inverse estimates of anthropogenic CO_2 uptake, transport, and storage by the ocean. Global Biogeochem. Cycles 20 (2), n/a–n/a. https://doi.org/10.1029/2005GB002530.

Miller, L.A., Burgers, T.M., Burt, W.J., Granskog, M.A., Papakyriakou, T.N., 2019. Air-Sea CO_2 Flux Estimates in Stratified Arctic Coastal Waters: How Wrong Can We Be? Geophys. Res. Lett. 46 (1), 235–243. https://doi.org/10.1029/2018GL080099.

Miller, L.A., Carnat, G., Else, B.G.T., Sutherland, N., Papakyriakou, T.N., 2011a. Carbonate system evolution at the Arctic Ocean surface during autumn freeze-up. J. Geophys. Res. Ocean. 116 https://doi.org/10.1029/2011JC007143.

Miller, L.A., Papakyriakou, T.N., Collins, R.E., Deming, J.W., Ehn, J.K., Macdonald, R.W., Mucci, A., Owens, O., Raudsepp, M., Sutherland, N., Papakyriakou, N., Collins, R.E., Deming, J.W., Ehn, J.K., Macdonald, R.W., Mucci, A., Owens, O., Raudsepp, M., Sutherland, N., 2011b. Carbon dynamics in sea ice: A winter flux time series. J. Geophys. Res 116, 2028. https://doi.org/10.1029/2009JC006058.

Miller, S., Marandino, C., Saltzman, E.S., 2010. Ship-based measurement of air-sea CO_2 exchange by eddy covariance. J. Geophys. Res. 115, D02304. https://doi.org/10.1029/2009JD012193.

Miller, S.D., Marandino, C.A., DeBruyn, W.J., Saltzman, E.S., 2009. Eddy correlation carbon dioxide and dimethlysulfide air-sea gas exchange in the North Atlantic. Geophys. Res. Lett 36, L15816.

Morison, J.H., McPhee, M.G., Curtin, T.B., Paulson, C.A., 1992. The Oceanography of Winter Leads. J. Geophys. Res. 97 (C7), 11199–11218.

Oelke, C., 1997. Atmospheric signatures in sea-ice concentration estimates from passive microwaves: Modelled and observed. Int. J. Remote Sens. 18 (5), 1113–1136. https://doi.org/10.1080/014311697218601.

Papakyriakou, T., Miller, L., 2011. Springtime CO_2 exchange over seasonal sea ice in the Canadian Arctic Archipelago. Ann. Glaciol. 52 (57), 215–224. https://doi.org/10.3189/172756411795931534.

Park, J.-W., Korosov, A., Babiker, M., Kim, H.-C., 2019. Automated Sea Ice Classification Using Sentinel-1 Imagery, in: IGARSS 2019 - 2019 IEEE International Geoscience and Remote Sensing Symposium. IEEE, pp. 4008–4011. Doi: 10.1109/IGARSS.2019.8898730.

Parkinson, C.L., 2019. A 40-y record reveals gradual Antarctic sea ice increases followed by decreases at rates far exceeding the rates seen in the Arctic. Proc. Natl. Acad. Sci. U. S. A. 116 (29), 14414–14423. https://doi.org/10.1073/pnas.1906556116.

Pereira, R., Ashton, I., Sabbaghzadeh, B., Shutler, J.D., Upstill-Goddard, R.C., 2018. Reduced air-sea CO_2 exchange in the Atlantic Ocean due to biological surfactants. Nat. Geosci. 11 (7), 492–496. https://doi.org/10.1038/s41561-018-0136-2.

Prytherch, J., Brooks, I.M., Crill, P.M., Thornton, B.F., Salisbury, D.J., Tjernström, M., Anderson, L.G., Geibel, M.C., Humborg, C., 2017. Direct determination of the air-sea CO_2 gas transfer velocity in Arctic sea ice regions. Geophys. Res. Lett. 44 (8), 3770–3778. https://doi.org/10.1002/2017GL073593.

Prytherch, J., Yelland, M.J., 2021. Wind, Convection and Fetch Dependence of Gas Transfer Velocity in an Arctic Sea-Ice Lead Determined From Eddy Covariance CO_2 Flux Measurements. Global Biogeochem. Cycles 35 (2). https://doi.org/10.1029/2020GB006633.

Rutgers van der Loeff, M.M., Cassar, N., Nicolaus, M., Rabe, B., Stimac, I., 2014. The influence of sea ice cover on air-sea gas exchange estimated with radon-222 profiles. J. Geophys. Res. Ocean. 119 (5), 2735–2751. https://doi.org/10.1002/2013JC009321.

Semiletov, I., Makshtas, A., Akasofu, S.-I., L Andreas, E., 2004. Atmospheric CO_2 balance: The role of Arctic sea ice. Geophys. Res. Lett. 31 (5), n/a–n/a.

Semiletov, I.P., Pipko, I.I., Repina, I., Shakhova, N.E., 2007. Carbonate chemistry dynamics and carbon dioxide fluxes across the atmosphere-ice-water interfaces in the Arctic Ocean: Pacific sector of the Arctic. J. Mar. Syst. 66 (1-4), 204–226. https://doi.org/10.1016/j.jmarsys.2006.05.012.

Serreze, M.C., Barry, R.G., 2011. Processes and impacts of Arctic amplification: A research synthesis. Glob. Planet. Change 77 (1-2), 85–96. https://doi.org/10.1016/j.gloplacha.2011.03.004.

Serreze, M.C., Stroeve, J., 2015. Arctic sea ice trends, variability and implications for seasonal forecasting. Philos. Trans. R. Soc. A Math. Phys. Eng. Sci. 373 (2045), 20140159. https://doi.org/10.1098/rsta.2014.0159.

Shutler, J.D., Land, P.E., Piolle, J.F., Woolf, D.K., Goddijn-Murphy, L., Paul, F., Girard-Arduin, F., Chapron, B., Donlon, C.J., 2016. FluxEngine: A flexible processing system for calculating atmosphere-ocean carbon dioxide gas fluxes and climatologies. J. Atmos. Ocean. Technol. 33, 741–756. https://doi.org/10.1175/JTECH-D-14-00204.1.

Shutler, J.D., Wanninkhof, R., Nightingale, P.D., Woolf, D.K., Bakker, D.CE., Watson, A., Ashton, I., Holding, T., Chapron, B., Quilfen, Y., Fairall, C., Schuster, U., Nakajima, M., Donlon, C.J., 2020. Satellites will address critical science priorities for quantifying ocean carbon. Front. Ecol. Environ. 18 (1), 27–35. https://doi.org/10.1002/fee.2129.

Sievers, J., Sørensen, L.L., Papakyriakou, T., Else, B., Sejr, M.K., Haubjerg Søgaard, D., Barber, D., Rysgaard, S., 2015. Winter observations of CO_2 exchange between sea ice and the atmosphere in a coastal fjord environment. Cryosph. 9, 1701–1713. https://doi.org/10.5194/tc-9-1701-2015.

Smeets, C.J.P.P., Broeke, M.R., 2008. Temporal and spatial variations of the aerodynamic roughness length in the ablation zone of the greenland ice sheet. Boundary-Layer Meteorol. 128 (3), 315–338. https://doi.org/10.1007/s10546-008-9291-0.

Sørensen, L.L., Jensen, B., Glud, R.N., McGinnis, D.F., Sejr, M.K., Sievers, J., Søgaard, D. H., Tison, J.L., Rysgaard, S., 2014. Parameterization of atmosphere-surface exchange of CO_2 over sea ice. Cryosphere 8, 853–866. https://doi.org/10.5194/tc-8-853-2014.

Spreen, G., Kern, S., 2017. Chapter 9 Methods of satellite remote sensing of sea ice. In: Thomas, D.N. (Ed.), *Sea Ice*, 3rd Edition. Wiley-Blackwell, ISBN 978-1-118-77838-8, pp. 239–260. https://doi.org/10.1002/9781118778371.

Stammerjohn, S.E., Martinson, D.G., Smith, R.C., Yuan, X., Rind, D., 2008. Trends in Antarctic annual sea ice retreat and advance and their relation to El Niño-Southern Oscillation and Southern Annular Mode variability. J. Geophys. Res. 113 (C3) https://doi.org/10.1029/2007JC004269.

Stephens, B.B., Keeling, R.F., 2000. The influence of antarctic sea ice on glacial-interglacial CO_2 variations. Nature 404 (6774), 171–174. https://doi.org/10.1038/35004556.

Stroeve, J.C., Kattsov, V., Barrett, A., Serreze, M., Pavlova, T., Holland, M., Meier, W.N., 2012. Trends in Arctic sea ice extent from CMIP5, CMIP3 and observations. Geophys. Res. Lett. 39 (16), n/a–n/a. https://doi.org/10.1029/2012GL052676.

Strong, C., Rigor, I.G., 2013. Arctic marginal ice zone trending wider in summer and narrower in winter. Geophys. Res. Lett. 40 (18), 4864–4868. https://doi.org/10.1002/grl.50928.

Takahashi, T., Sutherland, S.C., Wanninkhof, R., Sweeney, C., Feely, R.A., Chipman, D. W., Hales, B., Friederich, G., Chavez, F., Sabine, C., Watson, A., Bakker, D.C.E., Schuster, U., Metzl, N., Yoshikawa-Inoue, H., Ishii, M., Midorikawa, T., Nojiri, Y., Körtzinger, A., Steinhoff, T., Hoppema, M., Olafsson, J., Arnarson, T.S., Tilbrook, B., Johannessen, T., Olsen, A., Bellerby, R., Wong, C.S., Delille, B., Bates, N.R., de Baar, H.J.W., 2009. Climatological mean and decadal change in surface ocean pCO_2, and net sea-air CO_2 flux over the global oceans. Deep. Res. Part II Top. Stud. Oceanogr. 56 (8-10), 554–577. https://doi.org/10.1016/j.dsr2.2008.12.009.

Verykokou, S., Ioannidis, C., 2018. Oblique aerial images: a review focusing on georeferencing procedures. Int. J. Remote Sens. 39 (11), 3452–3496. https://doi.org/10.1080/01431161.2018.1444294.

Wanninkhof, R., 2014. Relationship between wind speed and gas exchange over the ocean revisited. Limnol. Oceanogr. Methods 12 (6), 351–362. https://doi.org/10.4319/lom.2014.12.351.

Wanninkhof, R., Asher, W.E., Ho, D.T., Sweeney, C., McGillis, W.R., 2009. Advances in Quantifying Air-Sea Gas Exchange and Environmental Forcing. Ann. Rev. Mar. Sci. 1 (1), 213–244. https://doi.org/10.1146/annurev.marine.010908.163742.

Watson, A.J., Schuster, U., Shutler, J.D., Holding, T., Ashton, I.G.C., Landschützer, P., Woolf, D.K., Goddijn-Murphy, L., 2020. Revised estimates of ocean-atmosphere CO_2 flux are consistent with ocean carbon inventory. Nat. Commun. 11, 1–6. https://doi.org/10.1038/s41467-020-18203-3.

Webb, E.K., Pearman, G.I., Leuning, R., 1980. Correction of flux measurements for density effects due to heat and water vapour transfer. Q. J. R. Meteorol. Soc. 106 (447), 85–100. https://doi.org/10.1002/qj.49710644707.

Weiss, A.I., King, J., Lachlan-Cope, T., Ladkin, R., 2011. On the effective aerodynamic and scalar roughness length of Weddell Sea ice. J. Geophys. Res. 116, D19119. https://doi.org/10.1029/2011JD015949.

Woolf, D.K., Land, P.E., Shutler, J.D., Goddijn-Murphy, L.M., Donlon, C.J., 2016. On the calculation of air-sea fluxes of CO_2 in the presence of temperature and salinity gradients. J. Geophys. Res. Ocean. 121 (2), 1229–1248. https://doi.org/10.1002/2015JC011427.

Woolf, D.K., Shutler, J.D., Goddijn-Murphy, L., Watson, A.J., Chapron, B., Nightingale, P. D., Donlon, C.J., Piskozub, J., Yelland, M.J., Ashton, I., Holding, T., Schuster, U., Girard-Ardhuin, F., Grouazel, A., Piolle, J.-F., Warren, M., Wrobel-Niedzwiecka, I., Land, P.E., Torres, R., Prytherch, J., Moat, B., Hanafin, J., Ardhuin, F., Paul, F., 2019. Key Uncertainties in the Recent Air-Sea Flux of CO 2. Global Biogeochem. Cycles 33 (12), 1548–1563. https://doi.org/10.1029/2018GB006041.

Yamamoto-Kawai, M., Mclaughlin, F., Carmack, E., Nishino, S., Shimada, K., 2009. Aragonite Undersaturation in the Arctic Ocean: Effects of Ocean Acidification and Sea Ice Melt. Science (New York, N.Y.). 326. doi:, 1098–1100. https://doi.org/10.1126/science.1174190.

Yang, M., Prytherch, J., Kozlova, E., Yelland, M.J., Parenkat Mony, D., Bell, T.G., 2016. Comparison of two closed-path cavity-based spectrometers for measuring air-water CO_2 and CH_4 fluxes by eddy covariance. Atmos. Meas. Tech. 9, 5509–5522. https://doi.org/10.5194/amt-9-5509-2016.

Yang, M., Smyth, T.J., Kitidis, V., Brown, I.J., Wohl, C., Yelland, M.J., Bell, T.G., 2021. Natural variability in air–sea gas transfer efficiency of CO_2. Sci. Rep. 11, 1–9. https://doi.org/10.1038/s41598-021-92947-w.

Yasunaka, S., Murata, A., Watanabe, E., Chierici, M., Fransson, A., van Heuven, S., Hoppema, M., Ishii, M., Johannessen, T., Kosugi, N., Lauvset, S.K., Mathis, J.T., Nishino, S., Omar, A.M., Olsen, A., Sasano, D., Takahashi, T., Wanninkhof, R., Omar, A.M., Lauvset, S.K., Watanabe, E., Kosugi, N., Olsen, A., Mathis, J.T., van Heuven, S., Ishii, M., Sasano, D., Murata, A., Fransson, A., Chierici, M., Nishino, S., Yasunaka, S., Takahashi, T., Hoppema, M., Johannessen, T., 2016. Mapping of the air–sea CO_2 flux in the Arctic Ocean and its adjacent seas: Basin-wide distribution and seasonal to interannual variability. Polar Sci. 10, 323–334. https://doi.org/10.1016/j.polar.2016.03.006.

Yasunaka, S., Siswanto, E., Olsen, A., Hoppema, M., Watanabe, E., Fransson, A., Chierici, M., Murata, A., Lauvset, S.K., Wanninkhof, R., Takahashi, T., Kosugi, N., Omar, A.M., Van Heuven, S., Mathis, J.T., 2018. Arctic Ocean CO 2 uptake: an improved multiyear estimate of the air-sea CO 2 flux incorporating chlorophyll a concentrations. Biogeosciences 15, 1643–1661. https://doi.org/10.5194/bg-15-1643-2018.

Zavarsky, A., Goddijn-Murphy, L., Steinhoff, T., Marandino, C.A., 2018. Bubble-Mediated Gas Transfer and Gas Transfer Suppression of DMS and CO_2. J. Geophys. Res. Atmos. 123 (12), 6624–6647. https://doi.org/10.1029/2017JD028071.

Zemmelink, H.J., Delille, B., Tison, J.L., Hintsa, E.J., Houghton, L., Dacey, J.W.H., 2006. CO_2 deposition over the multi-year ice of the western Weddell Sea. Geophys. Res. Lett. 33, L13606. https://doi.org/10.1029/2006GL026320.

Zhang, Q., Skjetne, R., 2018. Sea Ice Image Processing with MATLAB®. CRC Press.

Zhang, X., Zhu, Y., Zhang, J., Meng, J., Li, X., Li, X., 2020. An Algorithm for Sea Ice Drift Retrieval Based on Trend of Ice Drift Constraints from Sentinel-1 SAR Data. J. Coast. Res. 102, 113–126. https://doi.org/10.2112/SI102-015.1.

Spreen, G., Kaleschke, L., Heygster, G., 2008. Sea ice remote sensing using AMSR-E 89-GHz channel. J. Geophys. Res. Oceans 113 https://doi.org/10.1029/2005JC003384.